Pakistan J. Zool., pp 1-10, 2024. **DOI**: https://dx.doi.org/10.17582/journal.pjz/20231226090544

Studies on the Mitochondrial tRNA Gene Variants in Patients with Coronary Artery Disease and Pathogenicity Assessment by *in silico* Analysis

Fayaz Khan[1], Aziz Uddin[1], Hisham N. Altayb[2], Bibi Nazia Murtaza[3], Sajid Ul Ghafoor[1], Faisal Imam[4], Saima Iftikhar[5], Sadia Tabassum[1], Khushi Muhammad[1]* and Muhammad Shahid Nadeem[2]

[1]*Department of Biotechnology and Genetic Engineering, Hazara University, Mansehra, Pakistan.*
[2]*Department of Biochemistry, Faculty of Science, King Abdulaziz University, Jeddah, Saudi Arabia.*
[3]*Department of Zoology, Faculty of Science, Abbottabad University of Science and Technology, Abbottabad, Pakistan.*
[4]*Department of Pharmacology and Toxicology, College of Pharmacy, King Saud University, Riyadh, Saudi Arabia*
[5]*School of Biological Sciences, University of the Punjab, Lahore, Pakistan*

Article Information
Received 26 December 2023
Revised 21 February 2024
Accepted 06 March 2024
Available online 29 April 2024
(early access)

Authors' Contribution
FK, AU, SUG, MSN conceived the idea, prepared the research plan and contributed in the experimental process and data analysis. ST, FI, BNM, KM, revised manuscript. HNA carried out the *in silico* studies. SI analyzed data and prepared the manuscript.

Key words
Coronary artery disease, CAD, Mitochondrial tRNA genes, Mitochondrial dysfunction,

ABSTRACT

Mutations in mitochondrial DNA (mtDNA) have been associated with many pathological conditions including cardiovascular diseases. In the present study, we have evaluated the mutations in the mitochondrial tRNA genes for leucine, threonine and proline in patients with coronary artery disease (CAD). It included a large family with 11 cases and 29 healthy individuals. Mitochondrial tRNA genes were PCR amplified and analyzed for nucleotide sequences. Mutations were identified and the variants of genes were evaluated for structural variations by *in silico* analysis. Pathogenicity of individual tRNA variants was determined by molecular docking analysis and application of scoring systems such as MSeqDR, MitoTIP, HMTVar and PON-mt-tRNA. Four tRNA gene mutations including $tRNA^{Leu}$ (m.12285T>C, m.12308A>G), $tRNA^{Thr}$ (m.15928G>A), and $tRNA^{Pro}$ (m.15968T>C) were identified, m.12285 T>C and m.15968T>C being novel to CAD. Score based pathogenicity analysis of tRNA variants with MSeqDR, MitoTIP, HMTVar and PON-mt-tRNA have suggested that the variants were either likely or possibly polymorphic. Molecular docking studies of variants have shown significant difference in their structure, binding position and binding affinities with corresponding amino acyl tRNA synthetase. *In silico* results with structural abnormalities and molecular docking studies reflecting a failure of tRNA variants to bind the corresponding enzymes designate the potential role of identified variants in CAD pathogenicity. We have identified CAD specific variants in tRNA genes. These studies provide tRNA variants that can be applied for the early detection and screening of young populations for CAD.

INTRODUCTION

Defects in mitochondria lead to disorders such as learning disabilities, dementia, respiratory disorders, growth reduction, muscle failing, neurological issues, visual problems, loss of muscle coordination, heart diseases and hearing impairments (Nunnari and Suomalainen, 2012). Among the cellular organelles mitochondria are unique for their ability to produce energy in the form of ATP and perform many other cellular functions (Margineantu and Hockenbery, 2016). Mitochondrion is only organelle which is regulated synchronously by nuclear and its genome (Couvillion *et al*., 2016). Human mitochondrial genome is compact and no introns are present in the protein coding genes. The human mitochondrial genome is circular, double-stranded similar to that of a typical bacterium and consists of 16569 bp (D'Souza and Minczuk, 2018). Overall, there are 37 genes, 22 genes

* Corresponding author: khushi.muhammad@gmail.com
0030-9923/2024/0001-0001 $ 9.00/0

coded for tRNAs, 2 genes for rRNAs and 13 encoded for proteins. Approximately, 1500 mitochondrial proteins are encoded by the nuclear genome which contributes as the part of mitochondrial proteome (Heidari *et al*., 2022). The small mitochondrial genome is present as multiple copies in the cells which is maternally inherited (Palmer *et al*., 2021).

Having no histones (protective proteins), with limited repair capabilities, and being placed in close vicinity with the membrane associated with electron transport chain -the main source of reactive oxygen species (ROS), the mitochondrial genome is 10 to 20% more susceptible to mutations as compared to the nuclear genome (Lee *et al*., 2023). Human mitochondrial genome mutations lead to a broad range of disorders and defects in oxidative energy metabolism (Frazier *et al*., 2019). Some disorders are linked with somatic mutations such as ageing, cancer and neurodegenerative diseases (Young and Copeland, 2016). Pathogenic mitochondrial DNA mutations cause from 15% to 25% with abnormal oxidative phosphorylation (Kanungo *et al*., 2018). It has been investigated that protein synthesis by tRNA molecules and mutations make it possible to play a fundamental role in mitochondrial pathologies (DiMauro, 2019). There are reports describing the association of *tRNA* genes for proline, leucine and isoleucine with mitochondrial dysfunction and pathologies (Wang *et al*., 2016; Kraja *et al*., 2019). The mutations in *tRNA* genes cause a broad range of abnormalities for example gastrointestinal dysmotility, encephalopathy, cardiomyopathy and hearing loss (Suzuki, 2021).

Cardiovascular diseases (CVDs) represent a group of cardiac pathogenic conditions with defects in the blood circulatory system. Coronary artery disease (CAD), atherosclerosis and hypertension are rapidly growing pathologies (Mi *et al*., 2023). CAD is one of the most abundant CVDs affecting more than 100,000 people in China and 502,000 in the USA annually (Pencina *et al*., 2019; Abd El-Wahab, 2021). There are complicated associations of environmental factors, lifestyle and gene mutations to promote the disease pathology (Sliwa *et al*., 2024). Genome-wide study in central Asia and European countries identified numerous genetic loci which are associated with CAD (Wang *et al*., 2016; Heidari *et al*., 2022). CAD is one of maternally inherited common diseases having a link with mutations in mtDNA encoded tRNA genes. A specific mutation 15928G>A has been reported in up to 80% subjects with CAD (Ding *et al*., 2023). We have a systematic mutation screening project for the mtDNA of subjects from Northern Pakistani families suffering from epilepsy and heart diseases (Nadeem *et al*., 2019). The present study describes the study of a combined family of patients with CAD. The subjects with maternally transmitted CAD were selected from the Cardiac Clinic of DHQ Hospitals, Khyber Pakhtunkhwa, Pakistan. This study was designed the screening of mt tRNA genes for leucine 2, threonine, and proline (MT-TL2, MT-TT and MT-TP). Through *in silico* analysis, the impact of mutations was determined on the tRNA structures and their association with pathogenicity was evaluated.

MATERIALS AND METHODS

Enrollment of patients and families

It was analytical and cross sectional study and family having CAD patients were diagnosed through X-ray and ECG by professional doctors. The selected family members were notified about the aims and objectives of study. The consent form and questionnaire were filled by head of family to approve their contribution in an investigation and publication of data. For detailed information about cousin marriages and deceased members, a pedigree of family was constructed (Fig. 1). The details for each member of family about diseases and treatment were also recorded (Table I).

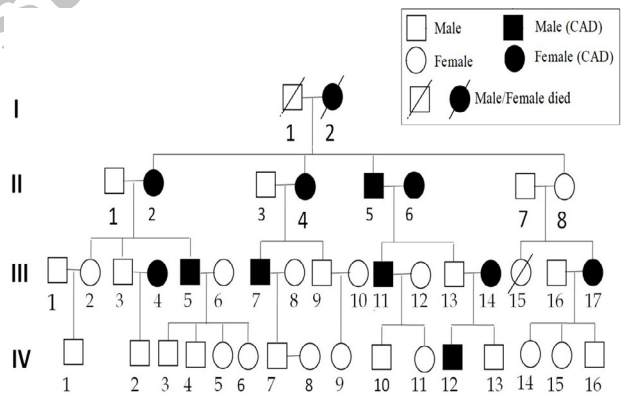

Fig. 1. A family pedigree with CAD. Affected individuals are indicated by filled symbols. An arrowhead denotes mutants.

Sampling and PCR amplification of target DNA

Blood samples were collected from the patients and other family members. DNA was extracted using Proteinase K and phenol chloroform based method. Nanodrop and gel electrophoresis procedures were performed to determine the quality and quantity of DNA. Finally, labelled samples were stored at -20ºC (Table II). The following set of primers were used for the PCR amplification of tRNA genes under optimized PCR conditions modified from the method provided with the PCR kit (Thermo Fisher catalogue No. 10572014).

Table I. Clinical and biochemical data for pedigrees of complete family.

Subjects	Gender	Age (Years)	Observation	Diagnosis	Systolic/ diastolic mm/Hg	LVD	RVD
II-1	M	90	N	N	130/85	45	20
II-2	F	80	CAD	ECG, X-ray	140/90	55	30
II-3	M	85	N	N	135/80	40	18
II-4	F	72	CAD	ECG, X-ray	140/90	52	26
II-5	M	75	CAD	ECG, X-ray	130/85	50	29
II-6	F	82	CAD	ECG, X-ray	140/90	53	28
II-7	M	70	N	N	145/95	40	12
II-8	F	78	N	N	130/90	38	15
III-1	M	62	N	N	125/83	39	13
III-2	F	59	N	N	122/81	37	16
III-3	M	63	N	N	140/90	42	15
III-4	F	58	CAD	ECG, X-ray	110/70	50	30
III-5	M	60	CAD	ECG, X-ray	125/82	55	29
III-6	F	56	N	N	120/90	50	20
III-7	M	50	CAD	ECG, X-ray	150/90	49	20
III-8	F	51	N	N	135/95	46	18
III-9	M	48	N	N	140/85	43	20
III-10	F	45	N	N	130/90	38	25
III-11	M	35	CAD	ECG, X-ray	140/90	52	25
III-12	F	30	N	N	135/85	47	18
III-13	M	30	N	N	130/90	41	17
III-14	F	27	CAD	ECG, X-ray	130/70	49	30
III-15	M	40	N	N	130/85	45	12
III-16	F	38	CAD	ECG, X-ray	150/95	50	26
IV-1	M	19	N	N	120/80	35	18
IV-2	M	25	N	N	120/85	37	20
IV-3	M	26	N	N	120/90	45	13
IV-4	M	24	N	N	120/80	39	12
IV-5	F	21	N	N	130/85	41	15
IV-6	F	19	N	N	120/90	47	14
IV-7	M	25	N	N	130/80	46	10
IV-8	F	20	N	N	120/85	40	18
IV-9	F	16	N	N	120/80	39	20
IV-10	M	22	N	N	125/80	37	25
IV-11	F	20	N	N	120/80	47	24
IV-12	M	15	CAD	ECG, X-ray	130/90	48	25
IV-13	M	13	N	N	120/80	39	16
IV-14	F	23	N	N	125/80	40	12
IV-15	F	20	N	N	120/85	43	9
IV-16	M	18	N	N	120/80	42	13

Table II. Primers for PCR amplification of the mt-tRNA genes. The primers were selected partly from D-Loop region to encompass tRNA gene with number of nucleotides sufficient for nucleotide sequence analysis.

Target gene	Primer ID	Primer sequence (5'-3')	Product size
tRNALou	MT-13F	TTTACCACAACACAATGGG	525bp
	R	GCTCAGTGTCAGTTCGAGATA	
tRNAT	MT-21F	ATCGGAGGACAACCAGTAAGC	320bp
	R	TGATGGGTGAGTCAATACTTGG	
tRNAPio	MT-22F	ATCGGAGGACAACCAGTAAGC	320bp
	R	TGATGGGTGAGTCAATACTTGG	

Detection of mutations by sequence analysis

The PCR products were analyzed by 1% agarose gel electrophoresis. Purified PCR products were commercially analyzed for nucleotide sequences from biological technology department of TSINGKE Chengdu (China). Further alignment studies were carried out through online DNA analysis tools like NCBI Blast and Ugene. The nucleotide sequences obtained were compared with rCRS (Revised Cambridge Reference Sequence).

Cross-validation of deleterious effect of mutations by computational tools

PON-mt-tRNA, a multi-factorial probability-based prediction tool, was used for classification of newly observed human mt-tRNA mutations. It integrates machine learning prediction with evidence of biochemistry, histochemistry, and segregation, to compute the posterior probability of pathogenicity. This method displayed high performance with Accuracy and Matthews Correlation Coefficient (MCC) of 1.00 and 0.99, respectively. It accepts input as the comma separated single query with mitochondrial genome location, reference nucleotide, and new nucleotide; output score ranges from 0 to 1, following increasingly deleterious pattern. Variations are classified into five classes that are, variants of uncertain significance, neutral, likely neutral, likely pathogenic, and pathogenic. Mitochondrial tRNA Informatics Predictor (MitoTIP, Philadelphia, PA, http://journals.plos.org/ploscompbiol/article? id=10.1371/ journal.pc bi.1005867), is another tool for predicting pathogenicity of novel mitochondrial tRNA variants, which was effectively employed in our analysis to have combinatorial optimization of *in silico* predictions. MitoTIP is based on multiple sources of information for prediction of the likelihood that novel single nucleotide variants in tRNA encoding sequences would cause disease (Nadeem *et al*., 2019; Sonney *et al*., 2017). Upon query, the predictive algorithm incorporates an estimation of the

importance of a position across all known mitochondrial tRNAs using data from publically available databases (like MITOMAP and GenBank); the output ranges from 5.9 to 21.8 (Supplementary data).

Secondary structure prediction of mutated genes

RNA structure webserver is a tool to predict RNA secondary structures with lowest free energy and base pair probabilities. The server to predict RNA secondary structure combines four separate prediction and analyzed algorithms which are, finding structures with the most predictable accuracy, expecting the lowest free energy structures, calculating the function separately and pseudoknot (if any) prediction. RNA sequence is taken by server and generates an extremely possible, annotated cluster of secondary structures, opening with the minimum free energy structure and including different probabilities of accuracy. Four mutant sequences (m.12285T>C, m.12308A>G, m.15928G>A and m.15968T>C) were submitted to the server for comparative structure analysis.

Prediction of RNA secondary and 3D structures

For the prediction of mitochondrial tRNA secondary structure, the RNAfold webserver (Lorenz *et al*., 2011), was used. The generated 2D structures were used in dot-bracket format for the generation of normal and mutant tRNA 3D structures using the automated RNA structure 3D Modeling server (RNA composer) was used for the prediction of mitochondrial tRNA 3D (Antczak *et al*., 2016; Rovcanin *et al*., 2020).

Protein 3D structures determination

The crystal structures of human tRNA synthetase were obtained from RCSB PDB, including the crystal structure of human prolyl-tRNA synthetase (PDB ID: 4HVC), the crystal structure of human threonyl-tRNA synthetase (PDB ID: 4HWT), and the crystal structure of human leucyl-tRNA synthetase (PDB ID: 6KIE). The 3D structures of tRNA synthetase were prepared for docking by the addition of hydrogen atoms, other hetero atoms were deleted. Ionization states were generated at pH 7.0 ± 2.0 using EPIK in Maestro. Eventually, water molecules were removed, and protein-energy was minimized using the OPLS3e force field (Roos *et al*., 2019).

Sequence and 3D structure alignment

The generated 3D of normal and mutant tRNA were aligned using Prime 2.0 interface in Maestro according to Schrodinger, LLC, New York, NY, USA) (Schrödinger, 2020), the superposition was used for structures alignment to all residues was used for alignment and root mean square deviation (RMSD) calculation.

Protein-RNA docking

The standard mode of protein and nucleic acid docking in Maestro was used for docking of mutant and normal tRNA with their corresponding tRNA synthetase with a maximum number of poses 30, the best poses were further analyzed for residues interaction using the fully automated Protein-Ligand Interaction Profiler (PLIP) (Salentin *et al*., 2015).

RESULTS

Subjects

In present study 40 individuals were enrolled from an interrelated family. All the investigated patients had symptoms of CAD and hypertension in their family history.

Genes and mutations

Analysis of the mt-tRNA genes in patients with CAD led us to identify 4 mutations: The nucleotide sequence analyses have indicated four point mutations including m.12285T>C, m.12308A>G, m.15928G>A and m.15968T>C (Fig. 2). The mutations m.12285T>C and m.15968T>C are new to literature, while the other two have been reported to represent the heteroplasmic condition.

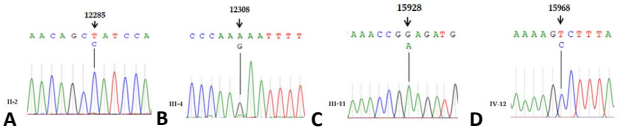

Fig. 2. The comparative analysis of affected with revised Cambridge Reference Sequence (rCRS) of human mitochondrial tRNA genes indicating mutations 12285T>C, 12308A>G, 15928G>A and 15968T>C.

Score based evaluation of tRNA variants for pathogenicity, validation by in silico *predictive tools*

Pathogenicity of mitochondrial tRNA variants was determined by MitoTIP and PON-mt-tRNA. For the evaluation of benign and pathogenic nature of tRNA variants MitoTIP (Mitochondrial tRNA Informatics Predictor) was applied (Sonney *et al*., 2017). The identified mt-tRNA variations were also classified by using the PON-mt-tRNA (a multifactorial probability-based prediction method) (Yarham *et al*., 2011; Niroula and Vihinen, 2016). All four variants were reported to be deleterious by MitoTIP and PON-mt-tRNA. The difference in the degree of predicted deleteriousness is due to the fact that both tools work on different algorithms/principles and consider diverse factors. However, the computational predictive tools strongly support that the mutations show different types of variation (Table III). The scores from both of the

Table III. List of mutations identified in CAD patients and their pathogenicity predictions by MSeqDR, MitoTIP, HMTVar and PON-mt-tRNA.

tRNA variants	MSeqDR		Mito TIP		PON-mt-tRNA		HMTVar	
	Score	Prediction	Score	Prediction	Score	Prediction	Score	Prediction
T12285C	0.200	Polymorphic	1.39	Likely benign	0.12	Neutral	0,30	Likely polymorphic
A12308G	0.00	Possibly pathogenic	11.85	Possibly benign	0.19	Likely Neutral	0.40	Likely pathogenic
G15928A	0.00	Possibly benign	2.46	Likely benign	0.41	Neutral	0.2	Polymorphic
T15968C	0.300	Polymorphic	7.54	Likely benign	0.13	Neutral	0.28	Likely polymorphic

above procedures were compared to determine the level of pathogenicity of variants identified in the present study (Table IV).

Table IV. Root Mean Square Deviation (RMSD) of normal and mutant tRNA aligned structures.

Variant	RMSD
tRNA ^{Pro} variant U13C	7.16 Å
tRNA ^{Leu} variant U20C	22.7 Å
tRNA ^{Leu2} variant A43G	2.5 Å
tRNA ^{Thr} variant G40A	3.75 Å

Predicted secondary structures of mt tRNA genes

The harmful impact of the variants nucleotide could be understood by particular secondary structure of mutant models. Two or three structures were generated by RNA structure webserver, in which one with minimum free energy was selected. Four mutant models that are, m.12285T>C, m.12308A>G, m.15928G>A and m.15968T>C were observed (Fig. 2), with disruptive confirmation that could change the role of mt.tRNA genes which lead to pathogenic phenotype (Figs. 3, 4).

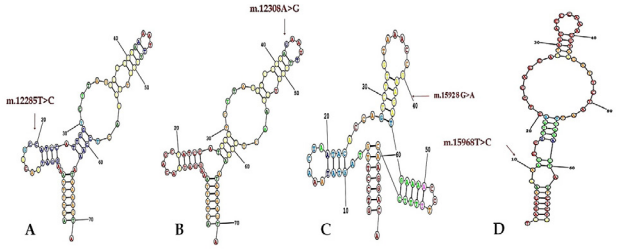

Fig. 3. Secondary and tertiary structures of tRNA variants indicating the mutations and 3D structure.

In silico *evaluation of mutated tRNA genes*

The generated 3D structures of normal and mutant tRNA were aligned by the Prime tool, as shown in (Fig. 4). The tRNA^{Leu2} variant U20C showed a big deviation from the normal structure with RMSD 22.7 Å, tRNA ^{Pro} variant U13C showed a high RMSD (7.16Å) when compared to the normal structure. The tRNA^{Leu2} variant A43G and ^{Thr} variant G40A showed the least deviation from normal structures with RMSD 2.5 and 3.75 Å, respectively (Table IV).

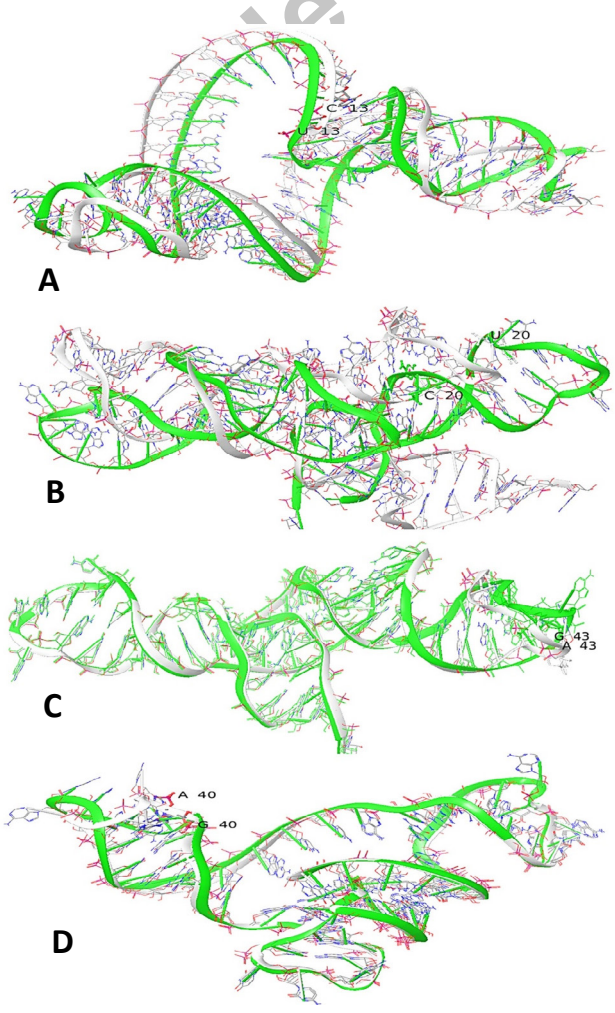

Fig. 4. Superimposition of normal (Green) and mutant (White) mtRNA (A). tRNA^{Pro} variant U13C (B). tRNA^{Leu2} variant U20C (C). tRNA^{Leu2} variant A43G (D). tRNA^{Thr} variant G40A.

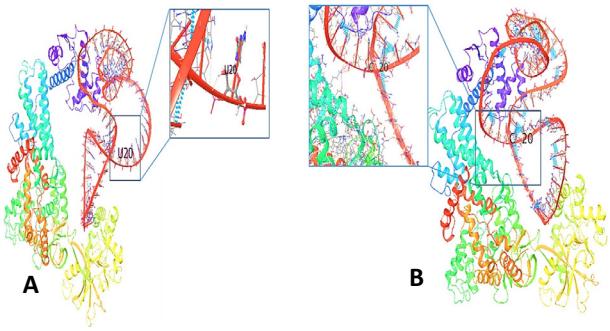

Fig. 5. 3D structure of the interaction of Leucyl- tRNA synthetase with $tRNA^{Leu2}$ (A). The normal with $tRNA^{Leu2}$ with a close-up view of the normal residue (U20) (B). The mutant with $tRNA^{Leu2}$ with a close-up view of the mutant residue (C20).

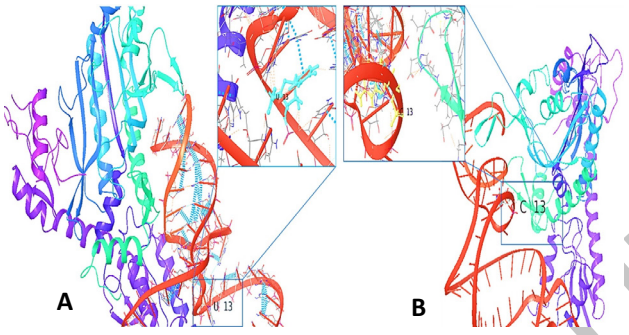

Fig. 6. 3D structure of the interaction of prolyl- tRNA synthetase with $tRNA^{Pro}$ (Red) (A). The normal $tRNA^{Pro}$ with close-up view of the normal residue (U13) (B). The mutant $tRNA^{Pro}$ (Red) with close-up view of the mutant residue (C13).

Molecular docking of tRNAs with aminoacyl-tRNA synthetase

Sequence alignment of normal and tRNA variants have shown four mutations resulting in $tRNA^{Leu}$ variant U20C, $tRNA^{Pro}$ variant U13C, $tRNA^{Leu}$ variant A43G, and $tRNA^{Thr}$ variant G40A (Table III; Supplementary Fig. S1). Molecular docking of normal and mutant tRNA showed a lot of differences in interaction and positioning of amino acyl synthetase and tRNAs. The molecular docking of normal (U20) and variant (C20) of $tRNA^{Leu}$ have shown significantly different pattern of interaction with Leucyl-tRNA synthetase (Fig. 5), (Supplementary Tables SI, SII and SIII). The normal $tRNA^{Pro}$, U13C, has shown 22 H-bonds with prolyl-tRNA, while the corresponding variant tRNA 13C has only 19 bonds. However, the binding pattern with enzyme was entirely different for both types of tRNA molecules (Fig. 6). The docking analysis of normal (A43) $tRNA^{Leu2}$ exhibited one hydrogen and two alkyl bonds with Lys965 of tRNA binding enzyme, with a small distance of 2.66Å, 2.20 Å, and 3.0 Å, respectively (Fig. 6). Simultaneously, the variant (G43) lacks the interaction with Leucyl- tRNA synthetase (Fig. 7). The threonyl-tRNA synthetase showed different interaction and positioning with its corresponding normal and mutant $tRNA^{Thr}$. Five H-bonds were unique with the normal $tRNA^{Thr}$, including Lys358 and C30, Leu691 and U13, Arg722 and A12, Val728 and A9, and Gln751 with C65. While the mutant $tRNA^{Thr}$ exhibited three unique H-bonds: Glu731 with A60, Arg740 with G62, and Lys750 A66 (Fig. 8).

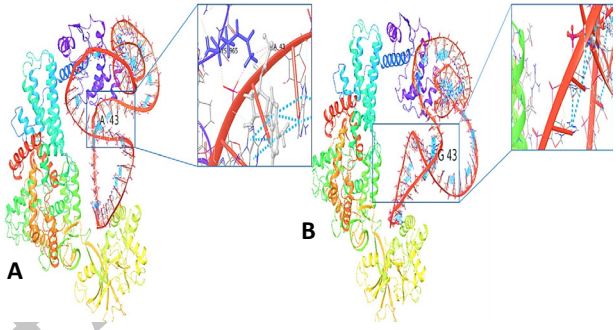

Fig. 7. 3D structure of the interaction of Leucyl- tRNA synthetase with $tRNA^{Leu2}$ (A) The normal with $tRNA^{Leu2}$ with a close-up view of the normal residue (A43) (B). The mutant with $tRNA^{Leu2}$ with a close-up view of the mutant residue (G43).

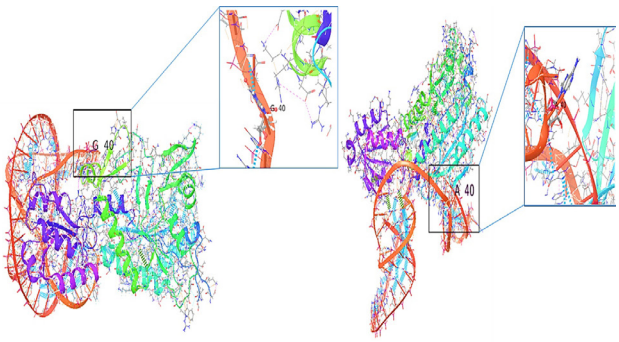

Fig. 8. 3D structure of the interaction of threonyl- tRNA synthetase with $tRNA^{Thr}$ (red) (A). The normal with $tRNA^{Thr}$ with a close-up view of the normal residue (G40) (B). The mutant with tRNA $tRNA^{Thr}$ with close-up view of the mutant residue (A40).

DISCUSSION

CVDs are the leading cause of human death worldwide (Benjamin *et al*., 2019). CAD is a serious threat to human health causing 1 out of 7 deaths in the USA (Thomas *et al*., 2021; Blumenthal *et al*., 2021). This is the

type of heart disease affecting about 25% of individuals globally and is the leading death cause in the western hemisphere (Sundaram *et al*., 2020). It leads to myocardial infarction, heart failure and sudden death that is recorded 50% in men and 64% in women. CAD has been associated with a combined or quantitative impact of multifactorial environmental conditions, psychological status and hereditary factors. Several risk factors associated with CAD include serum lipids, diabetes, blood ceramides, lifestyle and hypertension (Roth *et al*., 2019). Studies have established an association of family history and genetics with CAD, both factors may increase 40 to 60% chances of disease incidence. The genetic factors contribute to the quantitative polygenic effect in the development of CAD (Nikpay and Mohammadzadeh, 2020). Mitochondrial DNA mtDNA4977 deletion, 16189T>C, 15928G>A and T16519C have been associated with CAD (Heidari *et al*., 2020). Similarly, several tRNA gene mutations have been confirmed for associated pathogenicity in CAD patients (Kessler *et al*., 2021). We have evaluated a family with history of CAD for mt tRNA gene mutations (Fig. 1). A total of 40 individuals were recruited in the study after signing the consent forms, 11 of these subjects were diagnosed for CAD based on different diagnostic parameters and family history was recorded (Table I). Three genes $tRNA^{Leu}$, $tRNA^{Pro}$ and $tRNA^{Thr}$ were PCR amplified and fragment size was confirmed for each by agarose gel electrophoresis. Purified PCR products were commercially analyzed for nucleotide sequences and mutations in the above gene sequences were detected by peak correction. We identified $tRNA^{Leu}$ (m.12285T>C, m.12308A>G), $tRNA^{Thr}$ (m.15928G>A), and $tRNA^{Pro}$ (m.15968T>C) variants (Fig. 2). The variants m.12285 T>C and m.15968T>C are novel with respect to CAD and other two m.12308A>G and m.15968T>C have already been reported among the CAD patients (Heidari *et al*., 2020; Shemiakova *et al*., 2020). None of these mutations was detected in the healthy subjects from this family. The scores from MitoTIP and PON-mt-tRNA analysis were compared to determine the pathogenicity levels of variants identified in the present study (Table III). All four variants were found to be deleterious up to different levels (Din *et al*., 2021; Fu *et al*., 2021). RMSD (root mean square deviation) based comparison of normal and mutant *tRNA* genes by structural alignment analysis has shown significant structural differences between the normal and variant *tRNA* genes (Figs. 3, 4, and Table IV). The comparison between normal and mutant $tRNA^{Leu2}$ variant A43G and $tRNA^{Thr}$ variant G40A showed the least RMSD as compared to the variants $tRNA^{Pro}$ variant U13C and $tRNA^{Leu2}$ variant U20C, the last having major difference (Figs. 3, 4, Table IV). Usually, RMSD zero, indicates identical structures, and when this value increases, indicate structures become more different (Meng *et al*., 2021). Clear differences in the position of interaction between tRNA variants with the active site of amino acyl synthetase. Normal $tRNA^{Leu}$ (U20) and its identified variant (C20) have shown significant differences in interaction with Leucyl-tRNA synthetase (Fig. 5, Supplementary Tables SI, SII, SIII). Similarly, normal $tRNA^{Pro}$ (U13) and its corresponding identified variant $tRNA^{Pro}$ (13C) have shown different binding pattern with prolyl-tRNA (Fig. 6). Normal $tRNA^{Leu}$ (A43) has shown hydrogen and alkyl bonds with Lys^{965} of tRNA binding enzyme, with a distance of 2.66Å, 2.20 Å, and 3.0 Å, respectively (Fig. 7A). Simultaneously, the interaction of tRNA variant (43G) with Leucyl-tRNA synthetase is entirely different (Fig. 7B). Normal $tRNA^{Thr}$ (G40) has shown five H-bonds with the active site of corresponding enzyme. However, the variant $tRNA^{Thr}$ (40A) exhibited three unique H-bonds (Fig. 8). Hindrance in the proper binding of tRNA variants with their corresponding enzymes in the cellular systems has been associated with pathology of various conditions (Srinivas *et al*., 2021), including cardiovascular diseases (Ni *et al*., 2021).

CONCLUSION

The effect of known mutations on tRNA structure was estimated by online biological software and detailed *in silico* studies. The software based prediction studies have shown variable results, mostly indicating non-pathogenic effects of variants identified in the present study. However, the disruptive secondary and 3D structures of variants suggest mitochondrial dysfunction or pathogenic differences. Further studies for the *in vivo* confirmation of pathogenic role of these four tRNA gene variants are required.

Funding

The authors are grateful to the Researchers Supporting Project number (RSPD2024R939), King Saud University, Riyadh, Saudi Arabia for financial support.

IRB approval

The study was approved by Advanced Study and Research Board, Hazara University, Mansehra under notification number F.No.73/Ittl/ORlClB C2016/

Ethical statement

This study and its procedures were approved by Ethical Committee of Institution and Board of Advanced Studies and Research at Hazara University, Mansehra 21300, Pakistan according to the notification number

F.No.73/Ittl/ORIClB C2016/.

Supplementary material

There is supplementary material associated with this article. Access the material online at: https://dx.doi.org/10.17582/journal.pjz/20231226090544

Statement of conflicts of interest

The authors have declared no conflict o interest.

REFERENCES

Abd El-Wahab, E.W., 2021. Predicting coronary heart disease using risk assessment charts and risk factor categories. *J. Publ. Hlth.*, **29**: 1037-1045. https://doi.org/10.1007/s10389-020-01224-z

Antczak, M., Popenda, M., Zok, T., Sarzynska, J., Ratajczak, T., Tomczyk, K., Adamiak, R.W. and Szachniuk, M., 2016. New functionality of RNA composer: Application to shape the axis of miR160 precursor structure. *Acta Biochim. Pol.,* **63**: 737-744. https://doi.org/10.18388/abp.2016_1329

Benjamin, E.J., Muntner, P., Alonso, A., Bittencourt, M.S., Callaway, C.W., Carson, A.P., Chamberlain, A.M., Chang, A.R., Cheng, S., Das, S.R. and Delling, F.N., 2019. Heart disease and stroke statistics - 2019 update: A report from the American Heart Association. *Circulation*, **139**: e56-28. https://doi.org/10.1161/CIR.0000000000000659

Blumenthal, D.M., Howard, S.E., Como, J.S., O'Keefe, S.M., Atlas, S.J., Horn, D.M., Wagle, N.W., Wasfy, J.H., Yeh, R.W. and Metlay, J.P., 2021. Prevalence of Angina among primary care patients with coronary artery disease. *JAMA Netw. Open*, **4:** e2112800-e2112800. https://doi.org/10.1001/jamanetworkopen.2021.12800

Couvillion, M.T., Soto, I.C., Shipkovenska, G. and Churchman, L.S., 2016. Synchronized mitochondrial and cytosolic translation programs. *Nature*, **533**: 499-503. https://doi.org/10.1038/nature18015

D'Souza, A.R. and Minczuk, M., 2018. Mitochondrial transcription and translation: Overview. *Essays Biochem*., **62**: 309-320. https://doi.org/10.1042/EBC20170102

DiMauro, S., 2019. A brief history of mitochondrial pathologies. *Int. J. mol. Sci.*, **20**: 5643. https://doi.org/10.3390/ijms20225643

Din, A.U., Ghafoor, S.U., Akbar, F., Akhtar, N., Khan, M.F., Ullah, Z. and Kareem, A., 2021. Analysis of mutations in leu tRNA gene in patients of heart diseases. *Saudi J. biol. Sci.*, **29**: 436-443. https://doi.org/10.1016/j.sjbs.2021.09.010

Ding, Y., Yu, J., Gao, B. and Huang, J., 2023. Correlation of mitochondrial tRNA variants with coronary heart disease in a Chinese pedigree. Zhonghua yi xue yi chuan xue za zhi= Zhonghua yixue yichuanxue zazhi= *Chinese J. med. Genet*., **40**: 807-814.

Frazier, A.E., Thorburn, D.R. and Compton, A.G., 2019. Mitochondrial energy generation disorders: genes, mechanisms, and clues to pathology. *J. biol. Chem.*, **294**: 5386-5395. https://doi.org/10.1074/jbc.R117.809194

Fu, Y., Ricciardiello, F., Yang, G., Qiu, J., Huang, H., Xiao, J., Cao, Z., Zhao, F., Liu, Y., Luo, W., Chen, G., 2021. The role of mitochondria in the chemoresistance of pancreatic cancer cells. *Cells*, **10**: 497. https://doi.org/10.3390/cells10030497

Heidari, M.M., Khatami, M., Kamalipour, A., Kalantari, M., Movahed, M., Emmamy, M.H., Hadadzadeh, M., Bragança, J., Namnabat, M. and Mazrouei, B., 2022. Mitochondrial mutations in protein coding genes of respiratory chain including complexes IV, V, and mt-tRNA genes are associated risk factors for congenital heart disease. *Excli J.* (eCollection 2022), **21**: 1306.

Heidari, M.M., Mirfakhradini, F.S., Tayefi, F., Ghorbani, S., Khatami, M. and Hadadzadeh, M., 2020. Novel point mutations in mitochondrial MT-CO_2 gene may be risk factors for coronary artery disease. *Appl. Biochem. Biotechnol.,* **191**: 1331-1339. https://doi.org/10.1007/s12010-020-03275-0

Kanungo, S., Morton, J., Neelakantan, M., Ching, K., Saeedian, J. and Goldstein, A., 2018. Mitochondrial disorders. *Annls Transl. Med.*, **6**: 475. https://doi.org/10.21037/atm.2018.12.13

Kessler, T. and Schunkert, H., 2021. *Coronary artery disease genetics enlightened by genome-wide.* https://doi.org/10.1016/j.jacbts.2021.04.001

Kraja, A.T., Liu, C., Fetterman, J.L., Graff, M., Have, C.T., Gu, C., Yanek, L.R., Feitosa, M.F., Arking, D.E., Chasman, D.I. and Young, K., 2019. Associations of mitochondrial and nuclear mitochondrial variants and genes with seven metabolic traits. *Am. J. Hum. Genet.*, **104**: 112-138.

Lee, W., Zamudio-Ochoa, A., Buchel, G., Podlesniy, P., Marti Gutierrez, N., Puigròs, M., Calderon, A., Tang, H.Y., Li, L., Mikhalchenko, A. and Koski, A., 2023. Molecular basis for maternal inheritance of human mitochondrial DNA. *Nat. Genet.*, **55**: 1632-1639. https://doi.org/10.1038/s41588-023-01505-9

Lorenz, R., Bernhart, S.H., Siederdissen, C.H., Tafer, H., Flamm, C., Stadler, P.F. and Hofacker, I.L., 2011. Vienna RNA package 2.0. *Algorithms Mol.*

Biol., **6**: 1-14. https://doi.org/10.1186/1748-7188-6-26

Margineantu, D.H. and Hockenbery, D.M., 2016. Mitochondrial functions in stem cells. *Curr. Opin. Genet. Dev.,* **38:** 1101-1117. https://doi.org/10.1016/j.gde.2016.05.004

Meng, F., Zhou, M., Xiao, Y., Mao, X., Zheng, J., Lin, J., Lin, T., Ye, Z., Cang, X., Fum Y. and Wang, M., 2021. A deafness-associated tRNA mutation caused pleiotropic effects on the m1G37 modification, processing, stability and aminoacylation of tRNAIle and mitochondrial translation. *Nucl. Acids Res.,* **49:** 1075-1093. https://doi.org/10.1093/nar/gkaa1225

Mi, Y., Xue, Z., Qu, S., Yin, Y., Huang, J., Kou, R., Wang, X., Luo, S., Li, W. and Tang, Y., 2023. The economic burden of coronary heart disease in mainland China. *Publ. Hlth.*, **224**: 140-151. https://doi.org/10.1016/j.puhe.2023.08.034

Nadeem, M.S., Ahmad, H., Mohammed, K., Muhammad, K., Ullah, I., Baothman, O.A., Ali, N., Anwar, F., Zamzami, M.A. and Shakoori, A.R., 2018. Identification of variants in the mitochondrial lysine-tRNA (MT-TK) gene in myoclonic epilepsy pathogenicity evaluation and structural characterization by *in silico* approach. *J. cell. Biochem.*, **119**: 6258-6265. https://doi.org/10.1002/jcb.26857

Ni, M., Black, L.F., Pan, C., Vu, H., Pei, J., Ko, B., Cai, L., Solmonson, A., Yang, C., Nugent, K.M. and Grishin, N.V., 2021. Metabolic impact of pathogenic variants in the mitochondrial glutamyl-tRNA synthetase EARS2. *J. Inherit. Metabol. Dis*., **44**: 949-960. https://doi.org/10.1002/jimd.12387

Nikpay, M. and Mohammadzadeh, S., 2020. Phenome-wide screening for traits causally associated with the risk of coronary artery disease. *J. Hum. Genet*., **65**: 371-380. https://doi.org/10.1038/s10038-019-0716-z

Niroula, A. and Vihinen, M., 2016. PON-mt-tRNA: A multifactorial probability-based method for classification of mitochondrial tRNA variations. *Nucl. Acids Res*., **44**: 2020-2027. https://doi.org/10.1093/nar/gkw046

Nunnari, J. and Suomalainen, A., 2012. Mitochondria: In sickness and in health. *Cell*, **148**: 1145-1159. https://doi.org/10.1016/j.cell.2012.02.035

Palmer, C.S., Anderson, A.J. and Stojanovski, D., 2021. Mitochondrial protein import dysfunction: Mitochondrial disease, neurodegenerative disease and cancer. *FEBS Let.*, **595**: 1107-1131. https://doi.org/10.1002/1873-3468.14022

Pencina, M.J., Navar, A.M., Wojdyla, D., Sanchez, R.J., Khan, I., Elassal, J., D'Agostino Sr, R.B., Peterson, E.D. and Sniderman, A.D., 2019. Quantifying importance of major risk factors for coronary heart disease. *Circulation*, **139**: 1603-1611. https://doi.org/10.1161/CIRCULATIONAHA.117.031855

Release, S., 2020. 2: Prime; Schrödinger, LLC: New York, NY, USA, 2020.

Roos, K., Wu, C., Damm, W., Reboul, M., Stevenson, J.M,, Lu, C., Dahlgren, M.K., Mondal, S., Chen, W., Wang, L., Abel, R., 2019. OPLS3e: Extending force field coverage for drug-like small molecules. *J. Chem. Theory Comp*., **15**: 1863-1874. https://doi.org/10.1021/acs.jctc.8b01026

Roth, GA., Mensah. G.A., Johnson, C.O., Addolorato, G., Ammirati, E., Baddour, L.M., Barengo, N.C., Beaton, A.Z., Benjamin, E.J., Benziger, C.P. and Bonny, A., 2020. Global burden of cardiovascular diseases and risk factors, 1990–2019: Update from the GBD 2019 study. *J. Am. College Cardiol.,* **76**: 2982-3021.

Rovcanin, B., Jancic, J., Samardzic, J., Rovcanin, M., Nikolic, B., Ivancevic, N., Novakovic, I. and Kostic, V., 2020. *In silico* model of mtDNA mutations effect on secondary and 3D structure of mitochondrial rRNA and tRNA in Leber's hereditary optic neuropathy. *Exp. Eye Res.,* **201**: 108277. https://doi.org/10.1016/j.exer.2020.108277

Salentin, S., Schreiber, S., Haupt, V.J., Adasme, M.F. and Schroeder, M., 2015. PLIP: Fully automated protein–ligand interaction profiler. *Nucl. Acids Res*., **43**: W443-W447. https://doi.org/10.1093/nar/gkv315

Schunkert, H., Ko¨nig, I.R., Kathiresan, S., Reilly, M.P., Assimes, T.L., Holm, H., Preuss, M., Stewart, A.F., Barbalic, M. and Gieger, C., 2011. Large-scale association analysis identifies 13 new susceptibility loci for coronary artery disease. *Nat. Genet.,* **43**: 333-338.

Schrödinger, LLC, 2020. LigPrep. Available at: https://www. schrodinger.com/ligprep. Accessed Dec 4, 2020

Shemiakova, T., Ivanova, E., Grechko, A.V., Gerasimova, E.V., Sobenin, I.A. and Orekhov, A.N., 2020. Mitochondrial dysfunction and DNA damage in the context of pathogenesis of atherosclerosis. *Biomedicines*, **8**: 166. https://doi.org/10.3390/biomedicines8060166

Sliwa, K., Viljoen, C.A., Stewart, S., Miller, M.R., Prabhakaran, D., Kumar, K., Thienemann, F., Piniero, D., Prabhakaran, P., Narula, J. and Pinto, F., 2024. Cardiovascular disease in low-and middle-

income countries associated with environmental factors. *Eur. J. Prevent. Cardiol.*, pp. zwad388. https://doi.org/10.1093/eurjpc/zwad388

Sonney, S., Leipzig, J., Lott, M.T., Zhang, S., Procaccio, V., Wallace, D.C. and Sondheimer, N., 2017. Predicting the pathogenicity of novel variants in mitochondrial tRNA with MitoTIP. *PLoS Comput. Biol.,* **13**: e1005867. https://doi.org/10.1371/journal.pcbi.1005867

Srinivas, P., Steiner, R.E. and Pavelich, I.J., Guerrero-Ferreira, R., Juneja, P., Ibba, M. and Dunham, C.M., 2021. Oxidation alters the architecture of the phenylalanyl-tRNA synthetase editing domain to confer hyperaccuracy. *Nucl. Acids Res.,* **49**: 11800–11809. https://doi.org/10.1093/nar/gkab856

Sundaram, V., Bloom, C., Zakeri, R., Halcox, J., Cohen, A., Bowrin, K., Briere, J.B., Banerjee, A., Simon, D.I., Cleland, J.G. and Rajagopalan, S., 2020. Temporal trends in the incidence, treatment patterns, and outcomes of coronary artersy disease and peripheral artery disease in the UK, 2006–2015. *Eur. Ocean Heart J.,* **41**: 1636-1649. https://doi.org/10.1093/eurheartj/ehz880

Suzuki, T., 2021. The expanding world of tRNA modifications and their disease relevance. *Nat. Rev. Mol. Cell Biol.,* **22**: 375-392. https://doi.org/10.1038/s41580-021-00342-0

Thomas, M., Jones, P.G., Arnold, S.V. and Spertus, J.A., 2021. Interpretation of the Seattle Angina Questionnaire as an outcome measure in clinical trials and clinical care: A review. *JAMA Cardiol.,* **6**: 593-599. https://doi.org/10.1001/jamacardio.2020.7478

Wang, L., Chen, J., Zeng, Y., Wei, J., Jing, J., Li, G., Su, L., Tang, X., Wu, T. and Zhou, L., 2016. Functional variant in the SLC22A3-LPAL2-LPA gene cluster contributes to the severity of coronary artery disease. *Arteriosclerosis, Thrombos. Vascul. Biol.*, **36**: 1989-1996. https://doi.org/10.1161/ATVBAHA.116.307311

Wang, Y., Zhou., XL., Ruan,, Z.R., Liu, R.J., Eriani, G. and Wang, E,D., 2016. Ahuman disease-causing point mutation in mitochondrial threonyl-tRNA synthetase induces both structural and functional defects. *J. biol. Chem.,* **291**: 6507-6520. https://doi.org/10.1074/jbc.M115.700849

Yarham, J.W., Al-Dosary, M., Blakely, E.L., Alston, C.L., Taylor, R.W., Elson, J.L. and McFarland, R., 2011. A comparative analysis approach to determining the pathogenicity of mitochondrial tRNA mutations. *Hum. Mutat.*, **32**: 1319-1325. https://doi.org/10.1002/humu.21575

Young, M.J. and Copeland, W.C., 2016. Human mitochondrial DNA replication machinery and disease. *Curr. Opin. Genet. Dev.,* **38**: 52-62. https://doi.org/10.1016/j.gde.2016.03.005

Pakistan J. Zool., pp 1-10, 2024. **DOI**: https://dx.doi.org/10.17582/journal.pjz/20231226090544

Supplementary Material

Studies on the Mitochondrial tRNA Gene Variants in Patients with Coronary Artery Disease and Pathogenicity Assessment by *in silico* Analysis

Fayaz Khan[1], Aziz Uddin[1], Hisham N. Altayb[2], Bibi Nazia Murtaza[3], Sajid Ul Ghafoor[1], Faisal Imam[4], Saima Iftikhar[5], Sadia Tabassum[1], Khushi Muhammad[1]* and Muhammad Shahid Nadeem[2]

[1]Department of Biotechnology and Genetic Engineering, Hazara University, Mansehra, Pakistan.
[2]Department of Biochemistry, Faculty of Science, King Abdulaziz University, Jeddah, Saudi Arabia.
[3]Department of Zoology, Faculty of Science, Abbottabad University of Science and Technology, Abbottabad, Pakistan.
[4]Department of Pharmacology and Toxicology, College of Pharmacy, King Saud University, Riyadh, Saudi Arabia
[5]School of Biological Sciences, University of the Punjab, Lahore, Pakistan

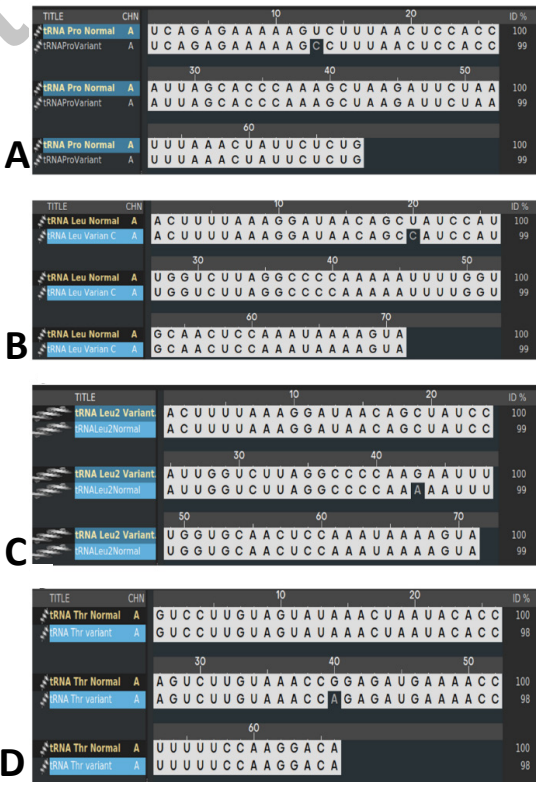

Supplementary Fig. S1. Sequence alignment of normal and mutant mtRNA the mutant residues are highlighted in black (A). $tRNA^{Pro}$ showing the variant U13C (B). $tRNA^{Leu2}$ variant U20C (C). $tRNA^{Leu2}$ variant A43G (D). $tRNA^{Thr}$ variant G40A.

* Corresponding author: khushi.muhammad@gmail.com
0030-9923/2024/0001-0001 $ 9.00/0

Supplementary Table SI. Comparison between the interaction of normal and mutant $tRNA^{PRO}$ and prolyl-tRNA synthetase.

Index	Normal					Mutant				
	Residue	AA	Distance H-A	Donor Atom	Acceptor Atom	Residue	AA	Distance H-A	Donor Atom	Acceptor Atom
1	1034R	LYS	2.17	305 (N3+)	7862 (O3)	1034R	LYS	3.11	305 (N3+)	7909 (O3)
2	1036R	GLU	1.84	9525 (Npl)	337 (O.co2)	1050R	ARG	1.97	563 (Ng+)	9526 (Npl)
3	1050R	ARG	2.86	563 (Ng+)	9513 (O-)	1050R	ARG	3.04	560 (Ng+)	9526 (Npl)
4	1054R	TYR	2.36	8255 (Nam)	636 (O3)	1052R	TRP	2.77	591 (Nam)	9559 (Npl)
5	1058R	GLU	2.49	8225 (Nam)	706 (O.co2)	1054R	TYR	1.79	636 (O3)	9481 (O-)
6	1061R	LYS	1.56	751 (N3+)	8224 (O2)	1331R	ARG	2.23	4983 (Ng+)	9595 (O3)
7	1075R	ASN	2.01	981 (Nam)	8275 (O-)	1342R	ARG	2.7	5193 (Ng+)	9564 (O3)
8	1147R	TRP	1.7	2124 (Nam)	8274 (O2)	1345R	LEU	1.69	5230 (Nam)	9640 (O2)
9	1342R	ARG	3.3	5193 (Ng+)	9530 (O3)	1346R	ARG	2.92	5258 (Ng+)	7970 (Npl)
10	1342R	ARG	2.96	5194 (Ng+)	9521 (N2)	1346R	ARG	2.32	5249 (Nam)	9640 (O2)
11	1345R	LEU	3.04	5230 (Nam)	9609 (O2)	1349R	TYR	2.35	7937 (Npl)	5310 (O3)
12	1346R	ARG	2.95	5258 (Ng+)	9523 (N2)	1349R	TYR	1.93	5310 (O3)	9746 (Npl)
13	1346R	ARG	3.48	5259 (Ng+)	9523 (N2)	1350R	SER	1.59	5325 (O3)	7858 (O-)
14	1348R	ASN	1.62	5292 (Nam)	9673 (O-)	1353R	TRP	1.87	5360 (Nar)	7906 (N2)
15	1349R	TYR	2.96	9492 (Npl)	5310 (O3)	1353R	TRP	2.51	5352 (Nam)	7858 (O-)
16	1349R	TYR	2.69	7937 (Npl)	5310 (O3)	1356R	ASN	1.71	5425 (Nam)	7890 (O2)
17	1349R	TYR	1.72	5310 (O3)	9715 (O2)	1361R	LYS	3.02	5515 (N3+)	9557 (N2)
18	1350R	SER	1.71	5325 (O3)	7791 (O-)					
19	1352R	GLY	2.67	5345 (Nam)	7790 (O2)					
20	1353R	TRP	1.94	5360 (Nar)	7872 (N2)					
21	1356R	ASN	1.67	5425 (Nam)	7857 (O2)					
22	1361R	LYS	2.96	5515 (N3+)	9530 (O3					

Supplementary Table SII. Comparison between the interaction of normal and mutant $tRNA^{THR}$ and threonyl-tRN synthetase.

Index	Normal			Mutant				
	Residue	AA	Distance H-A	Residue	AA	Distance H-A	Donor Atom	Acceptor Atom
1	354R	ARG	2.54	357T	ARG	3.3	65 (Ng+)	7760 (O3)
2	354R	ARG	3.05	357T	ARG	2.4	64 (Ng+)	7622 (N2)
3	354R	ARG	2.84	521T	SER	3.14	7053 (Npl)	2764 (O2)
4	354R	ARG	2.15	521T	SER	1.9	2766 (O3)	7012 (O3)
5	358R	LYS	3.68	526T	SER	1.93	2840 (O3)	7088 (N2)
6	526R	SER	2.59	582T	LYS	2.69	3733 (N3+)	7151 (N2)
7	526R	SER	2.38	526T	SE	3.08	3830 (O3)	7107 (O-)
8	582R	LYS	1.93	582T	LYS	1.69	5415 (O3)	6657 (O-)
9	582R	LYS	2.95	692T	ASN	1.79	5443 (Nam)	6657 (O-)
10	691R	LEU	2.55	696T	ARG	3.01	5529 (Ng+)	6581 (O3)
11	692R	ASN	1.95	726T	ASN	1.53	6018 (Nam)	6597 (O-)
12	692R	ASN	2.8	731T	GLU	1.94	6087 (Nam)	6800 (O2)
13	696R	ARG	3.31	696T	ARG	3.55	6109 (Ng+)	6830 (Npl)
14	696R	ARG	2.36	732T	ARG	1.62	6112 (Ng+)	6863 (O2)
15	722R	ARG	2.75	732T	ARG	2.38	6111 (Ng+)	6863 (O2)
16	726R	ASN	2.31	740T	ARG	2.11	6242 (Ng+)	6928 (N2)
17	728R	VAL	3.22	743T	GLN	1.71	6301 (Nam)	6947 (O-)
18	751R	GLN	3.06	749T	SER	2.92	6415 (O3)	6992 (Npl)
19	751R	GLN	3.27	750T	LYS	1.97	6429 (N3+)	7023 (O2)

Supplementary Table SIII. Comparison between the interaction of normal and mutant tRNA ^{Leu2} variant U20C, tRNA ^{Leu2} variant A43G and threonyl-tRNA synthetase.

Index	Normal			tRNA ^{Leu2} variant U20C					tRNA ^{Leu2} variant A43G				
	Residue	AA	Distance H-A	Residue	AA	Distance H-A	Donor Atom	Acceptor Atom	Residue	AA	Distance H-A	Donor Atom	Acceptor Atom
1	354R	ARG	2.54	357T	ARG	3.3	65 (Ng+)	7760 (O3)	262R	GLN	2.46	3625 (Nam)	17312 (O2)
2	354R	ARG	3.05	357T	ARG	2.4	64 (Ng+)	7622 (N2)	457R	ARG	2.35	6695 (Ng+)	17186 (O-)
3	354R	ARG	2.84	521T	SER	3.14	7053 (Npl)	2764 (O2)	473R	TYR	2	6978 (O3)	17377 (O2)
4	354R	ARG	2.15	521T	SER	1.9	2766 (O3)	7012 (O3)	512R	LYS	1.83	7602 (N3+)	17254 (N2)
5	358R	LYS	3.68	526T	SER	1.93	2840 (O3)	7088 (N2)	559R	ARG	1.56	8359 (Ng+)	17418 (O2)
6	526R	SER	2.59	582T	LYS	2.69	3733 (N3+)	7151 (N2)	559R	ARG	3.06	8360 (Ng+)	17418 (O2)
7	526R	SER	2.38	588T	TYR	3.08	3830 (O3)	7107 (O-)	907R	HIS	3.21	16722 (Npl)	13896 (Nar)
8	582R	LYS	1.93	690T	THR	1.69	5415 (O3)	6657 (O-)	907R	HIS	2.27	13893 (Nar)	16688 (O2)
9	582R	LYS	2.95	692T	ASN	1.79	5443 (Nam)	6657 (O-)	910R	ARG	2.49	13945 (Ng+)	16654 (N2)
10	691R	LEU	2.55	696T	ARG	3.01	5529 (Ng+)	6581 (O3)	914R	LYS	2.22	14029 (N3+)	16627 (N2)
11	692R	ASN	1.95	726T	ASN	1.53	6018 (Nam)	6597 (O-)	915R	ASN	1.96	16593 (Nam)	14046 (O2)
12	692R	ASN	2.8	731T	GLU	1.94	6087 (Nam)	6800 (O2)	966R	LEU	2.95	14614 (Nam)	17569 (O2)
13	696R	ARG	3.31	732T	ARG	3.55	6109 (Ng+)	6830 (Npl)	969R	ASN	1.7	14666 (Nam)	17637 (O3)
14	696R	ARG	2.36	732T	ARG	1.62	6112 (Ng+)	6863 (O2)	983R	LYS	2.02	18445 (Npl)	14871 (O2)
15	722R	ARG	2.75	732T	ARG	2.38	6111 (Ng+)	6863 (O2)	983R	LYS	1.63	14876 (N3+)	18025 (O2)
16	726R	ASN	2.31	740T	ARG	2.11	6242 (Ng+)	6928 (N2)	984R	LYS	1.67	14898 (N3+)	18061 (O3)
17	728R	VAL	3.22	743T	GLN	1.71	6301 (Nam)	6947 (O-)	987R	LYS	1.67	14958 (N3+)	18412 (O2)
18	751R	GLN	3.06	749T	SER	2.92	6415 (O3)	6992 (Npl)	1001R	GLU	3.46	17554 (O3)	15201(O.co2)
19	751R	GLN	3.27	750T	LYS	1.97	6429 (N3+)	7023 (O2)	1002R	LYS	2.36	15216 (N3+)	16818 (Nam)
20	965R	LYS	2.66	751R	GLN	1.99	6242 (Ng+)	6928 (N2)	100R	LYS2	2.40		